



**UNIVERSIDAD NACIONAL AUTONOMA
DE MEXICO**

Facultad de Medicina



INSTITUTO DE INVESTIGACIONES BIOMEDICAS

**EL COTRANSPORTADOR DE NA:CL ES ACTIVADO Y FOSFORILADO EN EL
DOMINIO AMINO-TERMINAL POR LA DEPLECION DE CLORURO INTRACELULAR**

LICENCIATURA EN INVESTIGACION BIOMEDICA BASICA

ABIGAIL DIAZ TELLEZ

DIRECTOR DE TESIS: DR. GERARDO GAMBA AYALA



MEXICO, D.F.

2007



Universidad Nacional
Autónoma de México

Dirección General de Bibliotecas de la UNAM

Biblioteca Central



UNAM – Dirección General de Bibliotecas
Tesis Digitales
Restricciones de uso

DERECHOS RESERVADOS ©
PROHIBIDA SU REPRODUCCIÓN TOTAL O PARCIAL

Todo el material contenido en esta tesis esta protegido por la Ley Federal del Derecho de Autor (LFDA) de los Estados Unidos Mexicanos (México).

El uso de imágenes, fragmentos de videos, y demás material que sea objeto de protección de los derechos de autor, será exclusivamente para fines educativos e informativos y deberá citar la fuente donde la obtuvo mencionando el autor o autores. Cualquier uso distinto como el lucro, reproducción, edición o modificación, será perseguido y sancionado por el respectivo titular de los Derechos de Autor.

A mí familia

INDICE

RESUMEN	1
INTRODUCCIÒN	2
METODOLOGIA	4
RESULTADOS Y DISCUSIÒN	7
REFERENCIAS	16
FIGURAS	19

The Na-Cl Cotransporter is Activated and Phosphorylated at the Amino Terminal Domain by Intracellular Chloride Depletion*

Diana Pacheco-Alvarez¹‡, Pedro San Cristóbal¹‡, Patricia Meade[‡], Erika Moreno^{‡§}, Norma Vazquez[‡], Abigail Díaz[‡], María Eugenia Juárez[‡], Ignacio Giménez[‡] and Gerardo Gamba²

‡Molecular Physiology Unit, Instituto Nacional de Ciencias Médicas y Nutrición Salvador Zubirán, Instituto de Investigaciones Biomédicas, Universidad Nacional Autónoma de México. Tlalpan 14000, Mexico City, Mexico. § Instituto de Ciencias de la Salud, Universidad Autónoma del Estado de Hidalgo, Pachuca, Hidalgo, Mexico and [±] Department of Pharmacology and Physiology, Facultad de Medicina, Universidad de Zaragoza, Zaragoza, Spain .

Running title: Regulation of rNCC by chloride and phosphorylation

The renal Na⁺:Cl⁻ cotransporter rNCC is mutated in human disease, is the therapeutic target of thiazide-type diuretics, and is clearly involved in arterial blood pressure regulation. rNCC belongs to electroneutral cation-coupled chloride cotransporter family (SLC12A) that has two major branches with inverse physiological functions and regulation: Na-driven cotransporters (NCC and NKCC1/2) that mediate cellular Cl⁻ influx are activated by phosphorylation whereas, K-driven cotransporters (KCCs) that mediate cellular Cl⁻ efflux are activated by dephosphorylation. A cluster of three threonine residues at the amino terminal domain have been implicated in the regulation of NKCC1/2 by intracellular chloride, cell volume, vasopressin and WNK/STE-20 kinases. Nothing is known however, about rNCC regulatory mechanisms. By using rNCC heterologous expression in *Xenopus laevis* oocytes, here we show, that two independent intracellular chloride depleting strategies increased rNCC activity by three-fold. The effect of both strategies was synergic and dose-dependent. Confocal microscopy of EGFP-tagged rNCC showed no changes in rNCC cell surface expression, while immunoblot analysis, using the R5-anti-NKCC1-phosphoantibody, revealed increased phosphorylation of rNCC amino terminal domain threonine residues T53 and T58. Elimination of these threonines together with serine residue S71 completely prevented rNCC response to intracellular chloride depletion. We conclude that rNCC is activated by a mechanism that involves amino terminal domain phosphorylation.

The renal $\text{Na}^+:\text{Cl}^-$ cotransporter (NCC or TSC, gene symbol: *SLC12A3*, Locus ID 6559) that is expressed at the apical membrane of mammalian distal convoluted tubule (DCT) represents the major salt transport pathway in this segment of the nephron (1-4). Its essential role in preserving the extracellular fluid volume and blood pressure has been established by the identification of inactivating mutations of the *SLC12A3* gene as the cause of Gitelman's disease (5;6), an inherited disorder featuring arterial hypotension, renal salt wasting, hypokalemic metabolic alkalosis, hypocalciuria, and hypomagnesemia. In addition, a defect in NCC regulation by serine/threonine kinases WNK1 and WNK4 has been implicated in the pathogenesis of a salt-dependent form of human hypertension, known as pseudohypaldosteronism type II (PHAII) (7;8), that features marked sensitivity to hydrochlorothiazide and a clinical picture that is a mirror image of Gitelman's disease (9). NCC is the pharmacological target of thiazide type diuretics that are currently recommended by the Joint National Committee (JNCVII) for the detection, evaluation, and treatment of high blood pressure as the first line treatment of arterial hypertension, either as the unique drug or in combination with other antihypertensive agents (10).

Despite the importance of NCC for cardiovascular and renal physiology, pharmacology and pathophysiology, little is known about mechanisms by which NCC activity is regulated.

NCC belongs to the super family of electroneutral cation-coupled chloride cotransporters (SLC12) from which seven members have been identified, at both functional and molecular level. NCC, together with two isoforms of the $\text{Na}^+:\text{K}^+:2\text{Cl}^-$ cotransporter, NKCC1 and NKCC2, compose the Na-driven branch (NKCCs), and four isoforms of the $\text{K}^+:\text{Cl}^-$ cotransporter compose the K-driven branch (KCCs). Because these cotransporters are involved in regulation of cell volume and/or in clamping the intracellular chloride concentration $[\text{Cl}^-]_i$, it has been proposed that their activity is regulated by changes in cell volume and/or $[\text{Cl}^-]_i$, by means of phosphorylation/dephosphorylation pathways (for review see (11-15)).

Several lines of evidence suggest that phosphorylation activates NKCCs and inhibits KCCs cotransporters, while dephosphorylation inhibits NKCCs and activates KCCs cotransporters. For instance, cell shrinkage, low intracellular chloride concentration, and protein phosphatase inhibitors activate NKCC1. Studies in this last cotransporter led to the identification of three amino terminal threonine residues that become phosphorylated under such stimulatory conditions (16;17). These threonine residues participate also in the stimulation of NKCC1 and NKCC2 by serine/threonine kinase WNK3 (18;19), or WNK1-WNK4/STE20 kinases pathway (20;21), as well as NKCC2 by vasopressin in thick ascending limb cells (22).

Little is known however, about NCC regulation. We have shown that rNCC is partially inhibited by cell swelling (23) or WNK4 (7), and is remarkably activated by WNK3 (19), suggesting that, like NKCC1 and NKCC2, NCC could be regulated by cell volume, $[\text{Cl}^-]_i$ or WNK kinases, at least in part, through phosphorylation of the conserved amino terminal domain threonine residues. Here we show that rNCC activity and amino terminal domain phosphorylation is increased by $[\text{Cl}^-]_i$ -depletion strategies. rNCC activation is completely prevented when the amino terminal domain threonine residues T53 and T58, and serine residue S71 are eliminated, suggesting that these amino acid residues are absolutely required for such regulation.

EXPERIMENTAL PROCEDURES

Clones and Mutagenesis.

We used the rat NCC and human KCC2 cDNA's that we previously cloned from rat kidney and human brain, respectively (24;25). All site directed mutations were introduced by using the Quickchange site directed mutagenesis system (Stratagene). Automatic DNA sequencing was used to confirm all mutations. All primers used for mutagenesis were custom made (Sigma).

Assessment of the $\text{Na}^+:\text{Cl}^-$ cotransporter function.

rNCC activity was assessed by functional expression in *Xenopus laevis* oocytes following our previously published protocols(23;26). Oocytes injected with water or rNCC cRNA (10 ng/oocyte) were exposed to two different conditions that promote a decrease in the $[\text{Cl}^-]_i$: low Cl^- hypotonic stress and/or coinjection with the $\text{K}^+:\text{Cl}^-$ cotransporter KCC2cRNA (10 ng/oocyte). After injection, oocytes were maintained during four days in isotonic ND96 (In mM: 96 NaCl, 2 KCl, 1.8CaCl₂, 1.0 MgCl₂, and 5.0 HEPES/Tris pH 7.4). The night before the uptake assay, oocytes were incubated in two different osmolar conditions: isotonic(ND96; ~210 mOsm/Kg H₂O) or low Cl^- hypotonic stress: 79 mM Na⁺ isethionate, 2 mM K⁺-gluconate, 1.8 mM Ca²⁺ gluconate, 1.0 mM Mg²⁺-gluconate, 5 mM HEPES, ~170 mOsm/Kg H₂O, pH 7.4).

Then, tracer ²²Na⁺ uptake (New England Nuclear) was assessed in oocytes exposed to isotonicity using our usual isotonic uptake solution (in mM 40 NaCl, 56 N-methyl-D-glucamine [NMDG]-Cl, 1.8 CaCl₂, 1.0 MgCl₂, 5.0 HEPES, pH7.4, 210 mOsm/Kg H₂O), containing 1mM ouabain, 0.1 mM amiloride, and 0.1 mM bumetanide, plus 2 μCi of ²²Na⁺ per ml. In contrast, uptake in oocytes exposed to low Cl^- hypotonic stress was assessed in a similar hypotonic uptake medium (in mM 40 NaCl, 38 N-methyl-D-glucamine [NMDG]-Cl, 1.8 CaCl₂, 1.0 MgCl₂, 5.0 HEPES, pH7.4, 170 mOsm/Kg H₂O), with the same drugs and tracer ²²Na⁺.

Thus, ²²Na⁺ uptake in oocytes injected with water, rNCC cRNA alone, rNCC + KCC2 cRNA or any rNCC mutant with or without KCC2 cRNA was assessed under both, regular isotonic and Cl^- -free hypotonic protocols. Tracer activity was determined for each oocyte dissolved in 10% SDS by β-scintillation counting.

Assessment of the rNCC expression at the oocytes plasma membrane.

Surface expression of wild type or mutant NCC (see below) was determined with confocal microscopy by assessing the surface fluorescence in *Xenopus* oocytes using an amino-terminus EGFP-NCC fusion construct that we have previously validated (7;19;27-29). In this construct, the enhanced green fluorescent protein (EGFP) was fused in frame to the amino terminal domain of NCC. *Xenopus* oocytes were microinjected with water as control or with EGFP-WT-rNCC or EGFP-mutant-rNCC cRNA.

Four days later, oocytes were monitored for EGFP fluorescence in the oocytes surface using a Zeiss laser scanning confocal microscope (objective lensx10, Nikon). Excitation and emission wavelengths used to visualize EGFP fluorescence were 488 nm and 515-565 nm, respectively. For densitometry analysis, the plasma membrane fluorescence was quantified by determining the pixel intensity around the entire oocytes circumference using Sigma ScanPro image analysis software.

NCC phospho-antibody studies.

We used the previously characterized R5 antibody (17) that was raised to detect phosphorylation of residues T184 and T189 in shark NKCC1, a generous gift from B. Forbush. In order for rNCC to be recognizable by the R5 antibody (see results and discussion), we constructed a rNCC single-mutant Y56H-NCC or a quadruple mutant L49Y-Y56H-I59M-V61A using custom primers. Oocytes injected with appropriate cRNA constructs were incubated in the same experimental solutions and for the same time as those described above for functional analysis. At the end of the incubation period, 4 oocytes per group were homogenized in 100 μ L ice-cold anti-phosphatase solution (in mM: 150 NaCl, 30 NaF, 5.0 EDTA, 15 Na_2HPO_4 , 15 Pyrophosphate, 20 HEPES, pH 7.2) with 1% Triton X-100 and a protease inhibitor cocktail. Then, homogenate was cleared by centrifugation and supernatants were subjected to western blotting. The equivalent to 6 μ L lysate was loaded per lane. The analysis was repeated four times and functional expression was assessed in parallel for each experiment.

***In vitro* cRNA translation.**

To prepare cRNA for microinjection, each of the wild-type or mutant cDNA was digested at the 3' end using Not I or Nhe I from New England Biolabs (Carlsbed, California) and cRNA was transcribed *in vitro*, using T7 RNA polymerase mMESSAGING MACHINESTM (Ambion) transcription system. cRNA product integrity was confirmed on agarose gels and concentration

was determined by absorbance reading at 260 nm(DU 640, Beckman, Fullerton, CA). cRNA was stored frozen in aliquots at -80°C until used

Data analysis.

All results presented are based in a minimum of two different experiments with at least 10 oocytes per group in each experiment. Statistical significance is defined as two-tailed, with $p < 0.05$, and the results are presented as mean \pm SEM. The significance of the differences between groups was tested by one-way ANOVA with multiple comparisons using Bonferroni's correction.

RESULTS AND DISCUSSION

NCC activity is increased by intracellular chloride depletion maneuvers.

Since the regulatory mechanisms controlling electroneutral cotransporters in their native tissues and in transfected cells, seem to operate in response, or to correct changes in intracellular chloride concentration (11), the present study tested such mechanisms of regulation for NCC. We used two different experimental strategies to induce a depletion of $[Cl^-]_i$. The first protocol was to compare the activity of rNCC in *X. laevis* oocytes injected with rNCC cRNA alone or together with of K^+Cl^- cotransporter KCC2 cRNA. We chose KCC2 because it is the K^+Cl^- cotransporter isoform that is significantly active in isotonic conditions when expressed in *X. laevis* oocytes (11;25), thus maintaining a continuous K^+Cl^- efflux over the incubation days before the uptake assays were performed. A similar approach was used in HEK-293 cells by Gillen and Forbush that analyzed the regulation of NKCC1 activity by intracellular chloride depletion induced by cotransfecting the cells with KCC1 (30).

The second protocol was the “low Cl^- hypotonic stress” in which rNCC-injected oocytes were incubated in a Cl^- -free, slightly hypotonic medium (170 mOsm/Kg H_2O) for several hours before the uptake assay. Low Cl^- hypotonic stress is known to induce a decrease in $[Cl^-]_i$ in several cells (16;17), including oocytes from *Rana pipens* (31). In addition, low Cl^- hypotonic stress in *X. laevis* oocytes induces the opening of Cl^- channels that promote Cl^- efflux (32).

Figure 1 depicts the effect of each protocol separately, or together, upon tracer $^{22}Na^+$ uptake in H_2O - or rNCC-injected oocytes. As we have previously shown (1;23;28), $^{22}Na^+$ uptake in water-injected oocytes was very small and not thiazide sensitive, indicating that *X. laevis* oocytes does not express endogenous activity of a Na^+Cl^- cotransporter. As shown in Figure 1, the minimum uptake observed in water injected oocytes was not affected by KCC2 cRNA injection or by low Cl^- hypotonic stress. $^{22}Na^+$ uptake in rNCC-injected oocytes incubated overnight in regular ND96 was 2840 ± 154 pmol/oocyte $^{-1}$ $4h^{-1}$. In contrast, $^{22}Na^+$ uptake in oocytes co-injected with rNCC and KCC2 cRNA that were incubated in similar isotonic conditions was 11757 ± 514 pmol/oocyte $^{-1}$ $4h^{-1}$ ($p < 0.001$).

In oocytes injected with rNCC alone, but exposed to low Cl^- hypotonic stress, $^{22}Na^+$ uptake was 12449 ± 974 pmol/oocyte $^{-1}$ $4h^{-1}$ ($p < 0.001$). Combination of both experimental protocols resulted in synergistic effect since $^{22}Na^+$ uptake in rNCC+KCC2 cRNA-injected oocytes

incubated over night in the Cl^- -free hypotonic medium was $16469 \pm 669 \text{ pmol} \cdot \text{oocyte}^{-1} \cdot \text{h}^{-1}$ ($p < 0.001$).

As shown in figure 2, in oocytes incubated in isotonic conditions or exposed to low Cl^- hypotonic stress, the effect of KCC2 cRNA co-injection upon rNCC activity was dose dependent. Increased amount of KCC2 cRNA injected was associated with increased activity of rNCC. Oocytes exposed to low Cl^- hypotonic stress exhibited higher basal activity and reached the plateau phase at lower KCC2 cRNA concentrations. Therefore, promoting intracellular chloride depletion by two different strategies resulted in increased activity of the renal $\text{Na}^+ : \text{Cl}^-$ cotransporter, suggesting that, as NKCC1, NCC can also be regulated by chloride-sensitive mechanisms.

Effect of Intracellular chloride depletion protocols upon rNCC phosphorylation.

Data with kinase/phosphatase pharmacological inhibitors suggest that members of the *SLC12A* family of cotransporters are regulated by phosphorylation/dephosphorylation pathways. Phosphorylation induced by cell shrinkage, low intracellular Cl^- , and protein phosphatase inhibitors, stimulate NKCCs and inhibit KCCs, while dephosphorylation induced by cell swelling, high intracellular Cl^- , and protein phosphatases (PPs), stimulate KCCs and inhibit NKCCs (11;13;14;33;34). However, direct phosphorylation has only been demonstrated so far for NKCC1 and NKCC2 (17;22;35). By using R5 antibody –a phospho-antibody that recognizes the phosphorylation of two amino terminal domain threonine residues in NKCC1 (T184, T189, shark sequence) (17) or NKCC2, it has been shown that activation of these cotransporters by low Cl^- hypotonic stress, cell shrinkage or coexpression with the WNK3 kinase is associated with phosphorylation of these conserved threonine residues in both, NKCC1 and NKCC2 (17-19;36;37).

Figure 3 A depicts the alignment of an amino terminal domain fragment among NKCCs containing the three threonine residues that have been identified as phosphorylation sites in shark NKCC1. The first two threonine, corresponding to T53 and T58 in rNCC are conserved. The third threonine residue is not conserved in NCC, but this position is occupied by a serine residue (S71). The sixteen amino acid residues from shark NKCC1 that were used to raise the R5-phosphoantibody (17) are indicated. As shown in Figure 3B, however, the R5-phosphoantibody is not able to detect the wild-type rNCC under any experimental conditions, either because these threonines are not phosphorylated in rNCC or because the epitope for R5 is somewhat altered. The major difference in the 16 residues peptide between NKCC1 and rNCC

is the non-conservative change of a histidine (H) for a tyrosine (Y) at position 56. In addition to this change, other differences between NKCC2 and NCC are L for Y at position 49, I for M at position 59, and V for A at position 61. Thus, to render rNCC recognizable by R5-phosphoantibody, we created the single rNCC-Y56H mutant and the quadruple L49Y-Y56H-I59M-V61A mutant (rNCC-4M). As shown in the R5 blot depicted in Fig 3B, a light signal of ~120 kDa was observed in proteins extracted from rNCC-Y56H or rNCC-4M-injected oocytes under basal conditions. The immunoreactivity was remarkably increased in proteins extracted from oocytes that were coinjected with KCC2 or exposed to low Cl^- hypotonic stress.

As shown in figure 4, functional expression analysis revealed that single substitution of the tyrosine 56 for histidine (rNCC-Y56H) or the quadruple substitution (rNCC-4M) did not affect either the basal activity of rNCC, or its activation by the coinjection with KCC2 or low Cl^- hypotonic stress. These observations suggest that activity of rNCC in basal conditions is associated with phosphorylation of the amino terminal domain threonine residues T53 and T58. The phosphorylation level was significantly increased by intracellular chloride depletion strategies that simultaneously increased the cotransporter activity. Thus, amino terminal phosphorylation of rNCC is associated with increased activity. Supporting this conclusion, we have observed that protein phosphatases inhibition is coupled with increased activity of rNCC. Incubation of rNCC-injected *X. laevis* oocytes with the protein phosphatase inhibitor calyculin A (100 nM) resulted in significant increase in rNCC-mediated $^{22}\text{Na}^+$ uptake from a value of $3961 \pm 209 \text{ pmol} \cdot \text{oocyte}^{-1} \cdot \text{h}^{-1}$ in rNCC control group in the absence of calyculin A, to a value of $5888 \pm 310 \text{ pmol} \cdot \text{oocyte}^{-1} \cdot \text{h}^{-1}$ in its presence (N=45; p<0.001).

Effect of intracellular chloride depletion protocols upon rNCC surface expression.

Increased activity of rNCC by coinjection of KCC2 or low Cl^- hypotonic stress could be due to the activation of cotransporter units that are already in the plasma membrane or to an increase in the amount of transporter units that reach the plasma membrane. To analyze these possibilities, we assessed in *X. laevis* oocytes the surface expression of the EGFP-rNCC construct that we have previously validated (27). We have shown that EGFP-NCC fluorescence in the oocytes surface co-localizes with the F-404 specific plasma membrane dye and that oocytes injected with EGFP-NCC exhibit significant thiazide-sensitive $^{22}\text{Na}^+$ uptake, indicating the EGFP-NCC fluorescence is located in the plasma membrane.

Thus, we have successfully use the EGFP-NCC construct to assess the effect of elimination of N-glycosylation sites (27), Gitelman's type mutations (29), single nucleotide polymorphisms(28), and the kinases WNK3 (19) and WNK4 (7) upon both the surface and functional expression of rena $\text{Na}^+:\text{Cl}^-$ cotransporter.

Because the fluorescence intensity is assessed in the confocal microscope using live oocytes, the same oocytes were then used to assess functional expression. Oocytes injected with EGFP-rNCC cRNA were exposed to both strategies as mention above and the surface expression was assessed by monitoring the EGFP fluorescence with a confocal microscope.

As shown in Figure 5A and 5B, surface expression analysis revealed similar fluorescence intensity at the surface of oocytes in all groups. However, as shown in Figure 5C, thiazide-sensitive $^{22}\text{Na}^+$ uptake in the same EGFP-rNCC-injected oocytes was increased by the intracellular Cl^- depletion strategies, similar to that observed for wild type rNCC (Fig. 1). The uptake observed in EGFP-rNCC cRNA injected oocytes of $987 \pm 105 \text{ pmol} \cdot \text{oocyte}^{-1} \cdot \text{h}^{-1}$ increased by co injection with KCC2 cRNA ($3518 \pm 687 \text{ pmol} \cdot \text{oocyte}^{-1} \cdot \text{h}^{-1}$; $p < 0.01$), by low Cl^- hypotonic stress ($3525 \pm 301 \text{ pmol} \cdot \text{oocyte}^{-1} \cdot \text{h}^{-1}$; $p < 0.05$), or by both maneuvers together ($5096 \pm 401 \text{ pmol} \cdot \text{oocyte}^{-1} \cdot \text{h}^{-1}$; $p < 0.01$). These observations suggest that increased activity of rNCC induced by co injection with KCC2 or low Cl^- hypotonic stress is due to stimulation of the cotransporter intrinsic activity, rather than by an increase in rNCC exocytosis containing vesicles.

Effect of replacing T53, T58, and S71 of rNCC with alanine.

To define the role of each of the three putative phosphorylation sites of the amino terminal domain in NCC basal activity and the response to intracellular chloride depletion protocols, we substituted these residues with alanine by site directed mutagenesis to create the single mutants T53A, T58A, and S71A, the double mutants T53-58A, T58-S71A, and T53-S71A, and the triple mutant T53-T58-S71A. Figure 6 shows the averaged results from several experiments in which *X.laevis* oocytes were injected with similar amounts of wild-type rNCC cRNA or each mutant's cRNA. $^{22}\text{Na}^+$ uptake in water injected oocytes was $249 \pm 18 \text{ pmol} \cdot \text{oocyte}^{-1} \cdot \text{h}^{-1}$ whereas in rNCC- cRNA-injected oocytes was $3432 \pm 156 \text{ pmol} \cdot \text{oocyte}^{-1} \cdot \text{h}^{-1}$. Elimination of any of the three potential phosphorylation sites resulted in a significant reduction of rNCC functional expression to various degrees. $^{22}\text{Na}^+$ uptake in oocytes injected with the single mutants T53A, T58A or S71AcRNA was 2486 ± 155 , 452 ± 39 , and $851 \pm 89 \text{ pmol} \cdot \text{oocyte}^{-1} \cdot \text{h}^{-1}$, respectively.

Thus, the percentage of reduction was 27% for T53A, 75% for S71A, and 100% for T58A. The effect of T53A and S71A was synergic, since any combination to produce double mutants resulted in complete abolishment of basal rNCC activity. Consequently, the triple mutant also exhibited no activity. These observations suggest that T53 and S71 are required to achieve the full basal activity of the cotransporter, while T58 appears to be absolutely necessary for rNCC to express basal activity. Interestingly, our observations with the rNCC single mutants are similar to those of shark NKCC1, but different to rabbit NKCC2. The NKCC1 activity was completely prevented by elimination of the threonine residue T189 and partially reduced by elimination of T184 and T202 (16).

In contrast, in rabbit NKCC2 elimination of each of these threonines only reduced the activity by ~20% (37). Therefore, the amino terminal domain phosphorylation sites are required to achieve basal activity in NKCC1 and NCC, but not in NKCC2.

Figure 7. shows the effect of single, double, or triple mutations upon the response of rNCC to both intracellular chloride depletion maneuvers. Figure 7A shows the effect of low chloride hypotonic stress, figure 7B the effect of co-injection with KCC2 cRNA and figure 7C both maneuvers together. In these experiments, the basal activity of T53A and S71A was reduced by ~20% and ~80%, respectively, whereas in any other mutant was completely prevented.

However, the single and double mutants exhibited increased thiazide-sensitive Na^+ uptake, after low Cl^- hypotonic stress or coinjection with KCC2 cRNA. As shown before, the effect of both maneuvers was synergic since the increase in the wild type and mutant cotransporters activity was higher when oocytes co-injected with wild type or mutant NCC cRNA and KCC2 cRNA were exposed to low Cl^- hypotonic stress. Interestingly, the double mutant T58, S71A was not activated by low Cl^- hypotonic stress alone or KCC2 cRNA co-injection alone, but was significantly activated by both together. In contrast, the triple mutant in which T53, T58, and S71 were substituted with alanine was not activated, even by both maneuvers together.

As shown in figure 8, when both maneuvers were applied together, the fold over control activity was: rNCC 2.9 ± 0.3 ; T53A 3.1 ± 0.4 ; T58A 3.4 ± 0.8 ; S71A 3.5 ± 0.3 ; T53-58A 2.7 ± 0.5 ; T53-S71A 4.4 ± 1.0 ; T58-S71A 2.7 ± 0.8 , and triple mutant 0.4 ± 0.1 . The only difference with wild type rNCC that reached significance was the triple mutant. These observations suggest that elimination of the three phosphorylation sites resulted in an rNCC that was neither functional in basal conditions, nor activated by the intracellular Cl^- depletions strategies.

In contrast, as long as one of the three phosphorylation sites is present, rNCC could be non-functional in basal conditions, but still be activated by intracellular chloride depletion.

Effect of replacing T53, T58, and S71 upon EGFP-rNCC surface and functional expression.

Because elimination of the three phosphorylation sites in the amino terminal domain alone or in combination resulted in a significant reduction of the cotransporter basal activity, we wanted to know the effect of these mutations upon surface expression of the cotransporter.

We thus introduced the triple mutation T53,T58,S71A into the EGFP-rNCC cDNA. *X. laevis* oocytes were injected with 25 ng of each clone cRNA and four days later the surface fluorescence intensity was assessed under confocal microscopy.

Then, the same oocytes were used for functional analysis by assessing the thiazide-sensitive $^{22}\text{Na}^+$ uptake. As shown in Figure 9, the surface expression of the triple mutant EGFP-rNCC, was similar to wild type EGFP-rNCC, while the functional expression was completely abolished. As a positive control, in the same experiment, a group of oocytes was injected with 25 ng of cRNA transcribed from the EGFP-rNCC double mutant N404, 424Q, in which both N-glycosylation sites of EGFP-rNCC were eliminated.

As we have previously reported (27), elimination of the N-glycosylation sites resulted in a cotransporter in which the surface expression is seriously reduced, and thus its activity. The observation that elimination of phosphorylation sites resulted in reduction of the cotransporter activity, without affecting the surface expression is consistent with the results in figure 5 in which activation of rNCC by intracellular chloride depletion was not associated with surface expression changes.

Taking together, the results of the present study show for the first time that the renal $\text{Na}^+:\text{Cl}^-$ cotransporter is regulated by intracellular chloride concentration through phosphorylation of the amino terminal domain and that the mechanism seems to be due to an increased turnover rate of the cotransporter rather than by increasing its expression in the plasmamembrane.

Due to the gradient of accompanying cation, the Na^+ -coupled chloride cotransporters NKCCs mediate Cl^- influx, whereas K^+ -coupled chloride cotransporters KCCs mediate Cl^- efflux.

Because intracellular concentration of Na^+ and K^+ are quickly restored by $\text{Na}^+:\text{K}^+:\text{ATPase}$, what the activity of electroneutral cation chloride cotransporters seems to modulate is the $[\text{Cl}^-]_i$.

For instance, in most cells, $[\text{Cl}^-]_i$ and thus, cell volume, is maintained by coordinated activity of NKCC1 and KCC1. It has been demonstrated in duck red blood cells that activity of these cotransporters is regulated by $[\text{Cl}^-]_i$ in such a way that low $[\text{Cl}^-]_i$ activates NKCC1 and inhibits KCC1, whereas high $[\text{Cl}^-]_i$ activates KCC1 and inactivates NKCC1 (38;39). In neurons, intracellular chloride concentration is defined by the ratio of NKCC1/KCC2 and these in turns define the type of response to neurotransmitters such as GABA that acts by opening Cl^- channels in postsynaptic membranes.

The excitatory effect of GABA in the prenatal period is due to increased NKCC1/KCC2 ratio, which results in increased $[\text{Cl}^-]_i$, whereas the inhibitory effect of GABA in the postnatal period can be explained by decreased NKCC1/KCC2 ratio that results in decreased $[\text{Cl}^-]_i$ (40-43). It has been clearly shown that modulation of NKCC1 by $[\text{Cl}^-]_i$ is mediated, at least in part, by phosphorylation of the amino terminal domain threonine residues shown in Figure 3 (17;36).

In addition, recent studies have shown that electroneutral cation chloride cotransporters are regulated by members of two serine/threonine kinase families known as WNK and STE20-related kinases also through phosphorylation of the amino terminal domain (18-20;44;45). First it was shown that STE-20-related kinases such as SPAK or OSR1 mediate functional activation of NKCC1 (44;46) by a process in which phosphorylation of the amino terminal domain threonine residues is implicated.

Later, Vitarriet al. (20) observed that WNK1 and WNK4 seems to activate SPAK and OSR1, which in turns phosphorylated the amino terminal domain of NKCC1. At the functional level, Gagnon et al. (45) also showed that WNK4 is able to increase the activity of NKCC1 only in the presence of SPAK or OSR1. Distorted modulation of NCC activity by WNK1 and WNK4 is implicated in the patho physiology of arterial hypertension in patients with PHAII (7;8). WNK4 inhibits the activity of NCC and the PHAII type mutations prevent this inhibition, thus releasing NCC that by its increasing activity produces arterial hypertension.

This hypothesis can explain the exquisite sensitivity to thiazide-type diuretics in PHAII patients (9). WNK1 seems to produce PHAII by its ability to regulate WNK4 activity (8;47;48). We have recently shown that WNK3, another member of the WNK family, is a powerful activator

of NCC, as well as NKCC1 and NKCC2 (18;19). The activation of NKCC1 and NKCC2 induced by WNK3 is also associated with increased phosphorylation of the amino terminal domain threonine residues shown in figure 3 (18;19).

In the present study we show that NCC activity is modulated by $[Cl^-]_i$ and that phosphorylation of the amino terminal domain threonine residues T53 and T58, and probably S71, is implicated, suggesting that modulation of NKCCs by $[Cl^-]_i$ and WNKs could be mediated by a common pathway. Supporting this possibility, it has been suggested that activity of WNK kinases is modulated by intracellular chloride. Xu et al. (49) identified WNK1 at the molecular level and observed that its activity was remarkably increased in the presence of NaCl.

Then, Lenertz et al. (48) showed that WNK1 is activated by NaCl and other osmotic challenges in a variety of cell lines, including distal convoluted kidney tubule cells, while it is not affected by short or long exposure to several hormones and by agents that modulate cell proliferation, suggesting that the major regulator of WNK kinases is cell ion strength, volume and/or intracellular ion concentrations. In this regard, Moriguchi et al. (21) have recently shown in HEK293 cells that both, WNK1 and SPAK/OSR1 kinases activity is increased when cells were exposed to low Cl^- hypotonic stress, suggesting that WNK1 behave as an activator of SPAK/OSR1 in response to a decrease in the $[Cl^-]_i$.

Supporting the observations in the present study, Moriguchi et al. (21) also observed in HEK293 cells transfected with T7-tagged mouse NCC, that amino terminal domain of NCC can be phosphorylated *in vitro* by WNK1/SPAK/OSR1 pathway and that phosphorylation level increases when cells were incubated under low Cl^- hypotonic stress, and decreased when the residues T53, T58, and S71 were eliminated. Thus, taking all these observations together it is reasonable to speculate that $[Cl^-]_i$ probably regulates WNKs and STE20 kinases activity that in turns modulate electroneutral cotransporters function.

In summary, we present evidences that rNCC can be activated by intracellular chloride depletion strategies such as co-expression with the $K^+ : Cl^-$ cotransporter KCC2 and/or exposure to low Cl^- hypotonic stress. The rNCC activation is associated with increased phosphorylation of the threonine residues 53 and 58 at the amino terminal domain, without changing the surface expression of the cotransporter. In addition, substituting T53, T58, and S71 residues with alanine renders rNCC inactive in basal conditions and insensitive to intracellular chloride

depletion, indicating that in addition to T53 and T58, the serine at the position 71 is also critical for rNCC regulation.

REFERENCES

1. Gamba, G., Saltzberg, S. N., Lombardi, M., Miyanoshita, A., Lytton, J., Hediger, M.A., Brenner, B.M., and Hebert, S.C. (1993) *Proc.Natl.Acad.Sci.USA***90**, 2749-2753
2. Ellison, D.H., Velazquez, H., and Wright, F.S. (1987) *Am.J.Physiol.(Renal Fluid Electrolyte Physiol.)***253**, F546-F554
3. Plotkin, M.D., Kaplan, M.R., Verlander, J.M., Lee, W-S., Brown, D., Poch, E., Gullans, S.R., and Hebert, S.C. (1996) *Kidney Int.***50**, 174-183
4. Costanzo, L.S. (1985) *Am.J.Physiol.(Renal Fluid Electrolyte Physiol.)***248**, F527-F535
5. Simon, D.B., Nelson-Williams, C., Johnson-Bia, M., Ellison, D., Karet, F.E., Morey-Molina, A., Vaara, I., Iwata, F., Cushner, H.M., Koolen, M., Gainza, F.J., Gitelman, H.J., and Lifton, R.P. (1996) *Nature Genetics***12**, 24-30
6. Mastroianni, N., Bettinelli, A., Bianchetti, M., Colussi, G., de Fusco, M., Sereni, F., Ballabio, A., and Casari, G. (1996) *Am.J.Hum.Genet.***59**, 1019-1026
7. Wilson, F. H., Kahle, K. T., Sabath, E., Lalioti, M. D., Rapson, A. K., Hoover, R. S., Hebert, S.C., Gamba, G., and Lifton, R. P. (2003) *Proc.Natl.Acad.Sci.U.S.A***100**, 680-684
8. Yang, C. L., Angell, J., Mitchell, R., and Ellison, D. H. (2003) *J.Clin.Invest***111**, 1039-1045
9. Mayan, H., Vered, I., Mouallem, M., Tzadok-Witkon, M., Pauzner, R., and Farfel, Z. (2002) *J.Clin.Endocrinol.Metab***87**, 3248-3254
10. Chobanian, A. V., Bakris, G. L., Black, H. R., Cushman, W. C., Green, L. A., Izzo, J. L., Jr., Jones, D. W., Materson, B. J., Oparil, S., Wright, J. T., Jr., and Roccella, E. J. (2003) *JAMA***289**, 2560-2571
11. Gamba, G. (2005) *Physiol Rev.***85**, 423-493
12. Hebert, S. C., Mount, D. B., and Gamba, G. (2004) *Pflugers Arch.***447**, 580-593
13. Flatman, P. W. (2002) *Biochim.Biophys.Acta***1566**, 140-151
14. Adragna, N. C., Fulvio, M. D., and Lauf, P. K. (2004) *J.Membr.Biol.***201**, 109-137
15. Lauf, P. K. and Adragna, N. C. (2000) *Cell Physiol Biochem.***10**, 341-354
16. Darman, R. B. and Forbush, B. (2002) *J.Biol.Chem.***277**, 37542-37550
17. Flemmer, A. W., Gimenez, I., Dowd, B. F., Darman, R. B., and Forbush, B. (2002) *J.Biol.Chem.***277**, 37551-37558
18. Kahle, K. T., Rinehart, J., De los Heros, P., Louvi, A., Meade, P., Vazquez, N., Hebert, S. C., Gamba, G., Gimenez, I., and Lifton, R. P. (2005) *Proc.Natl.Acad.Sci.U.S.A***102**, 16783-16788
19. Rinehart, J., Kahle, K. T., De los Heros, P., Vazquez, N., Meade, P., Wilson, F. H., Hebert, S. C., Gimenez, I., Gamba, G., and Lifton, R. P. (2005) *Proc.Natl.Acad.Sci.U.S.A***102**, 16777-16782
20. Vitari, A. C., Deak, M., Morrice, N. A., and Alessi, D. R. (2005) *Biochem.J.***391**, 17-24

21. Moriguchi, T., Urushiyama, S., Hisamoto, N., Iemura, S., Uchida, S., Natsume, T., Matsumoto, K., and Shibuya, H. (2005) *J.Biol.Chem.***280**, 42685-42693
22. Gimenez, I. and Forbush, B. (2003) *J.Biol.Chem.***278**, 26946-26951
23. Monroy, A., Plata, C., Hebert, S. C., and Gamba, G. (2000) *Am J Physiol Renal Physiol***279**,F161-F169
24. Gamba, G., Miyanoshta, A., Lombardi, M., Lytton, J., Lee, WS., Hediger, M.A., and Hebert, S.C.(1994) *J.Biol.Chem.***269**, 17713-17722
25. Song, L., Mercado, A., Vazquez, N., Xie, Q., Desai, R., George, A. L., Gamba, G., and Mount, D. B. (2002) *Brain Res.Mol.Brain Res.***103**, 91-105
26. Plata, C., Meade, P., Vazquez, N., Hebert, S. C., and Gamba, G. (2002) *J Biol.Chem.***277**, 11004-11012
27. Hoover, R. S., Poch, E., Monroy, A., Vazquez,N., Nishio, T., Gamba, G., and Hebert, S. C.(2003) *J.Am.Soc.Nephrol.***14**, 271-282
28. Moreno, E., Tovar-Palacio, C., De los Heros, P., Guzman, B., Bobadilla, N. A., Vazquez, N., Riccardi, D., Poch, E., and Gamba, G. (2004) *J Biol.Chem.***279**, 16553-16560
29. Sabath, E., Meade, P., Berkman, J., De los Heros, P., Moreno, E., Bobadilla, N. A., Vazquez, N., Ellison, D. H., and Gamba, G. (2004) *Am.J.Physiol Renal Physiol***287**, F195-F203
30. Gillen, C. M. and Forbush, III B. (1999) *Am.J.Physiol (Cell Physiol)***276**, C328-C336
31. Keicher, E. and Meech, R. (1994)*J.Physiol.***475**, 45-57
32. Ackerman, M.J., Wickman, K.D., and Clapham, D.E. (1994) *J.Gen.Physiol.***103**, 153-179
33. Flatman, P. W., Adragna, N. C., and Lauf, P. K. (1996) *Am J Physiol***271**, C255-C263
34. Starke, L. C. and Jennings, M. L. (1993)*Am J Physiol***264**, C118-C124
35. Lytle, C. and Forbush, III B (1992) *J.Biol.Chem.***267**, 25438-25443
36. Darman, R. B., Flemmer, A., and Forbush, B. (2001) *J Biol.Chem.***276**, 34359-34362
37. Gimenez, I. and Forbush, B. (2005) *Am.J.Physiol Renal Physiol***289**, F1341-F1345
38. Lytle, C. and Forbush, B., III (1996) *Am.J.Physiol***270**, C437-C448
39. Lytle, C. and McManus, T. (2002)*Am.J.Physiol Cell Physiol***283**, C1422-C1431
40. Lu, J., Karadsheh, M., andDelpire, E. (1999) *J Neurobiol.***39**, 558-568
41. Rivera, C., Voipio, J., Payne, J. A., Ruusuvuori, E., Lahtinen, H., Lamsa, K., Pirvola, U., Saarma, M., and Kaila, K (1999)*Nature***397**, 251-255
42. Delpire, E. (2000) *News Physiol Sci.***15**, 309-312
43. Mercado, A., Mount, D. B., and Gamba, G. (2004) *Neurochem.Res.***29**, 17-25
44. Dowd, B. F. and Forbush, B. (2003) *J.Biol.Chem.***278**, 27347-27353
45. Gagnon, K. B., England, R., and Delpire, E. (2005) *Am.J.Physiol Cell Physiol***290**, C134-C142-2006

46. Piechotta, K., Garbarini, N., England, R., and Delpire, E. (2003) *J.Biol.Chem.***278**, 52848-52856
47. Subramanya, A. R., Yang, C. L., Zhu, X., and Ellison, D. H. (2006) *Am.J.Physiol Renal Physiol***290**, F619-F624
48. Lenertz, L. Y., Lee, B. H., Min, X., Xu, B. E., Wedin, K., Earnest, S., Goldsmith, E. J., and Cobb, M. H. (2005) *J.Biol.Chem.***280**, 26653-26658
49. Xu, B., English, J. M., Wilsbacher, J. L., Stippec, S., Goldsmith, E. J., and Cobb, M. H. (2000) *J.Biol.Chem.***275**, 16795-16801

ACKNOWLEDGMENTS

We are grateful to members of the Molecular Physiology Unit for their suggestions and assistance. I.G. is a “Ramón y Cajal” Researcher. This study was presented in part at the 2004 RenalWeek of the American Society of Nephrology, San Louis, MO, and the 2006 Experimental Biology meeting in San Francisco, CA.

FOOTNOTES

Abbreviations used are: PHAII, pseudohypoaldosteronism type II; WNK, with no lysine=K. KCCs, K-Cl cotransporters. NKCCs Na-(K)-Cl cotransporters, rNCC, rat thiazide-sensitive Na-Cl cotransporter.

Figures

Figure 1. Effect of intracellular chloride depletion protocols upon rNCC activity.

Xenopus laevis oocytes were injected with water or 0.2 µg/µl of rNCC cRNA alone or together with 0.2 µg/µl of KCC2 cRNA, as stated. After four days of incubation in regular ND96, oocytes were incubated 16 hours in either regular ND96 (210 mOsm/kg H₂O) or a Cl⁻-free hypotonic medium (170 mOsm/kg H₂O), as stated. Next day ²²Na⁺ uptake was assessed in absence (open bars) or presence (closed bars) of 100 µM metolazone in uptake media containing 40 mM NaCl with similar osmolarity to which oocytes were exposed the night before (see methods). Figure shows combined results from five different experiments, with the mean ± SEM of 50 oocytes for each group. *Significantly different from the uptake observed in the control group of rNCC-injected oocytes incubated in ND96. **Significantly different from each strategy alone.

Figure 2. Dose- dependent effect of KCC2 cRNA upon NCC activity in oocytes.

Thiazide-sensitive ²²Na⁺ uptake in oocytes injected with rNCC cRNA exposed to regular isotonic conditions (closed circles) or to low Cl⁻ hypotonic stress (open circles) the night before that uptake experiments were performed. Oocytes were co-injected with increased concentration of KCC2 cRNA as stated. Figure shows combined results from two different experiments. * p<0.05 vs corresponding group not coinjected with KCC2 cRNA.

Figure 3. Effect of intracellular chloride depletion protocols upon rNCC phosphorylation.

A) Sequence alignment of an amino terminal domain fragment of shark NKCC1 and mammalian NKCC2 and NCC, as stated. The proposed phosphorylation sites are highlighted by boxes. The arrow shows the Y56 residue in rNCC. B) A representative immunoblot analysis of proteins extracted from *X. laevis* oocytes injected with water, wild type rNCC cRNA, the mutant rNCC-Y56H cRNA or the mutant rNCC-4M cRNA at 0.2 µg/µl using the R5-phosphoantibody raised against the 16 residue phosphorylated peptide of NKCC1 shown in A. Similar results were observed in five different experiments.

Figure 4. Effect of intracellular chloride depletion protocols upon rNCC activity in mutants rNCC-Y56H and rNCC-4M.

Functional expression and response to KCC2 co injection or low Cl^- hypotonic stress in oocytes injected with water, wild type rNCC cRNA, the mutant rNCC-Y56H cRNA, or the mutant rNCC-4M. Four days after injection $^{22}\text{Na}^+$ uptake was assessed in the absence (open bars) or presence (closed bars) of 100 μM metolazone in the uptake medium. A representative experiment from a single frog, with the mean \pm SEM of 10 oocytes for each group, is shown. Similar results have been observed in five different experiments, each one using oocytes from a different frog. *Significantly different from the uptake observed in the corresponding control group.

Figure 5. Effect of intracellular chloride depletion protocols upon EGFP-rNCC surface expression.

Oocytes were injected with water or 25 ng of wild type EGFP-rNCC cRNA with or without 10 ng/oocyte of KCC2 cRNA. Four days later oocytes were incubated overnight in either isotonic ND96 or Cl^- -free hypotonic medium. Next day, the oocytes surface fluorescence was visualized through a laser scanning confocal microscope and activity was assessed by tracer $^{22}\text{Na}^+$ uptake assay as described in methods section. A) Shows a representative confocal image of each group, as stated. B) Fluorescence intensity is expressed as mean \pm SE of 10 oocytes exposed to isotonicity (open bars) or hypotonicity (closed bars), with or without coinjection with KCC2 cRNA, as stated. C) $^{22}\text{Na}^+$ uptake was assessed in the absence (open bars) or presence (closed bars) of 100 μM metolazone in the uptake medium. *Significantly different from the uptake observed in the EGFP-rNCC control group.

Figure 6. Effect of elimination of T53, T58 and/or S71 of rNCC upon the rNCC basal function.

$^{22}\text{Na}^+$ Uptake in oocytes injected with wild type or mutants rNCC, as stated, in the absence (open bars) or presence (closed bars) of 100 μM metolazone. Each bar shows the mean \pm SEM

of 25 to 40 oocytes from three to five different experiments. *Significantly different from the uptake observed in wild type rNCC; $p < 0.01$.

Figure 7. Effect of elimination of T53, T58 and/or S71 of rNCC upon rNCC activation by intracellular chloride depletion protocols.

Low Cl^- hypotonic stress, B) co-injection with KCC2 cRNA, and C) both maneuvers together. In all figures, open bars represent $^{22}\text{Na}^+$ uptake in control oocytes; e.g, oocytes injected with rNCC cRNA or mutant rNCC cRNA and incubated the night before the uptake assay in isotonic ND96. Dashed bars represent rNCC or mutant NCC cRNA-injected oocytes exposed to intracellular chloride depletion maneuvers. *Significantly different from the uptake observed in the corresponding control. Each bar represents at least the mean \pm SEM of 20 oocytes from two different frogs.

Figure 8. Percentage of wild type or mutant rNCC activation by intracellular chloride depletion.

For each clone uptake observed in oocytes exposed to control conditions was taken as 100% and uptake observed in oocytes co-injected with wild type or mutant rNCC and KCC2 cRNA plus low Cl^- hypotonic stress was normalized to control group. Then, all percentages were divided by 100 to obtain the fold over control. *Significantly different to NCC group.

Figure 9. Effect of elimination of phosphorylation sites in the amino terminal domain of EGFP-rNCC upon surface and functional expression.

A) Representative confocal image of each group, as stated. B) Fluorescence intensity is expressed as mean \pm SE of 20 oocytes from two different experiments. C) Functional expression assessed by $^{22}\text{Na}^+$ uptake assay in absence (open bars) or presence (closed bars) of 100 μM metolazone. Oocytes were injected with the wild type or mutant EGFP-rNCC cRNA as stated. Functional expression assays were performed with the same oocytes that were used for fluorescence analysis in B. The EGFP-N404,424Q rNCC mutant, in which the two N-glycosylation sites have been eliminated, was used as control and was described previously (27). *Significantly different from wild type EGFP-rNCC.

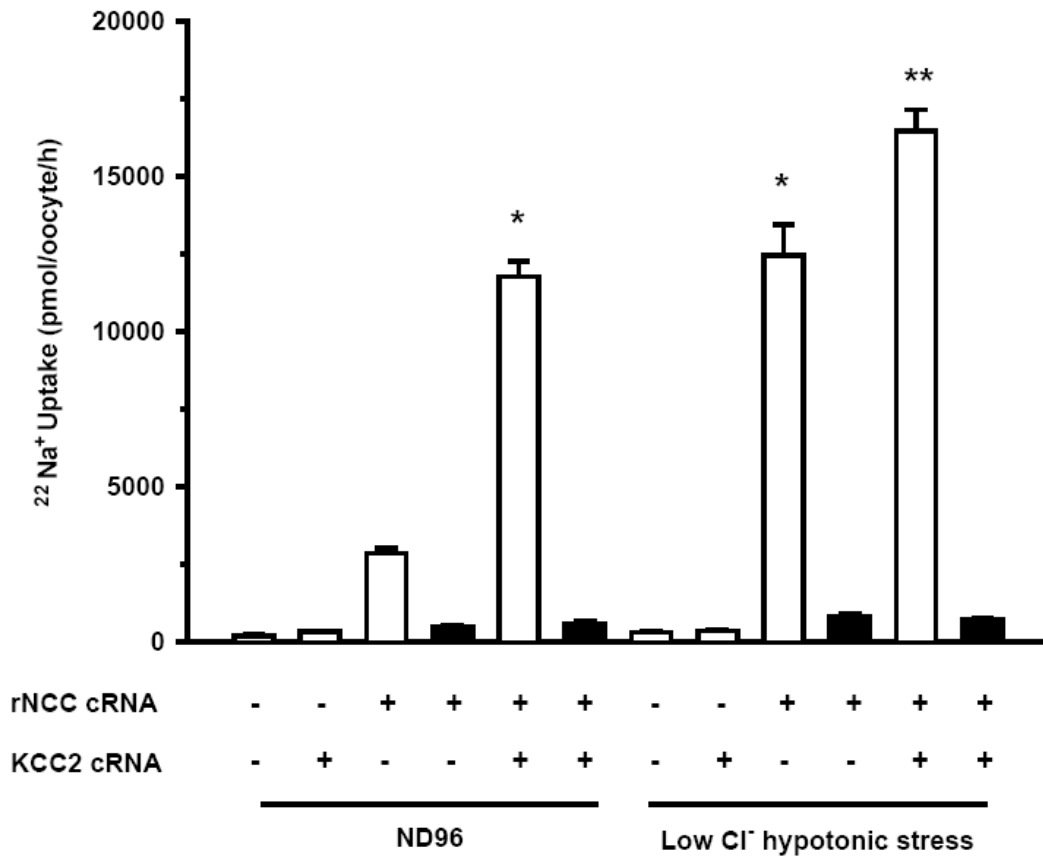


Figure 1

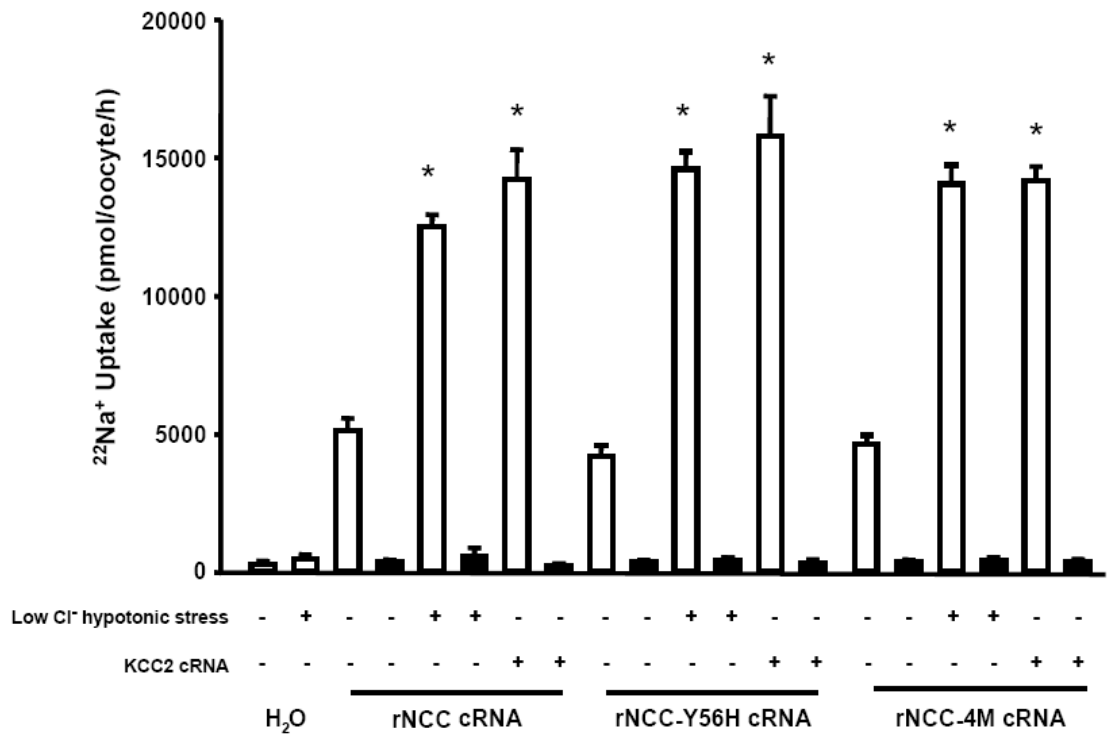


Figure 4

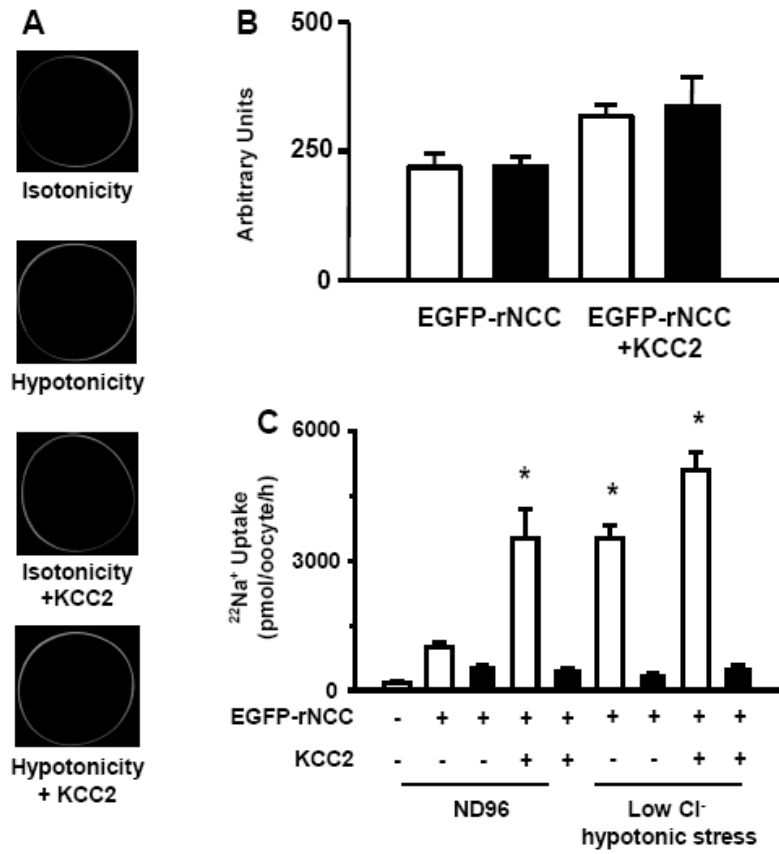


Figure 5

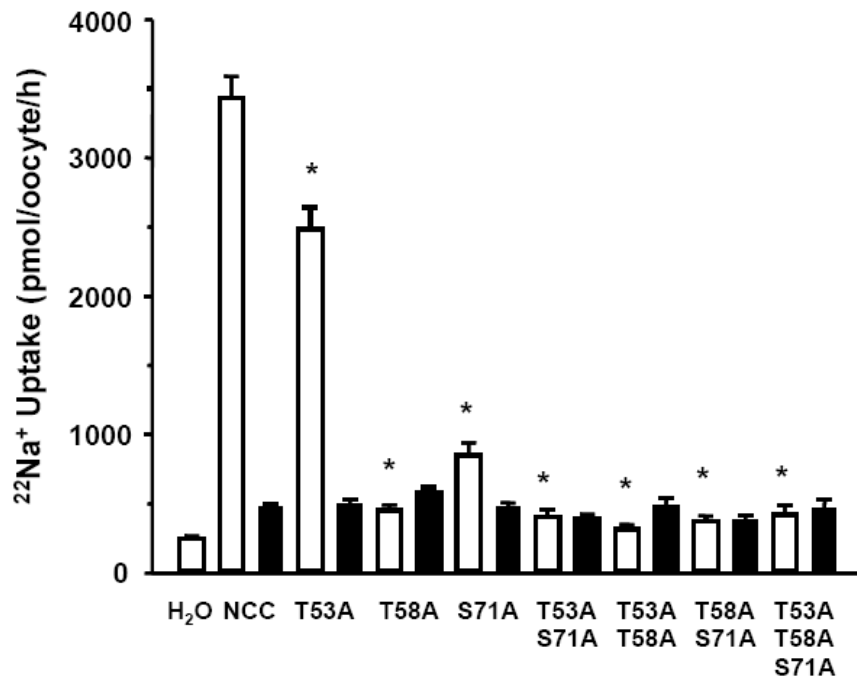


Figure 6

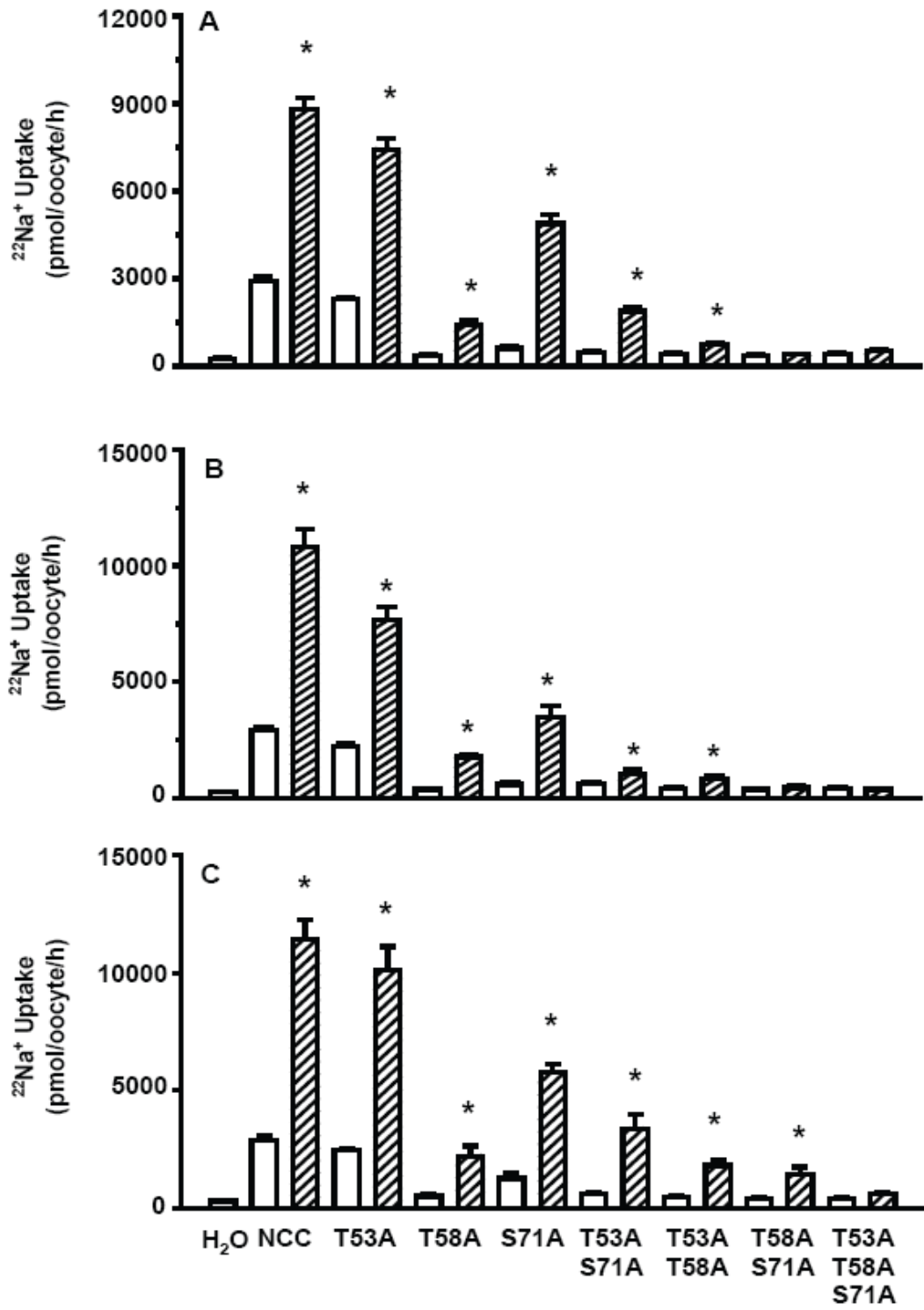


Figure 7

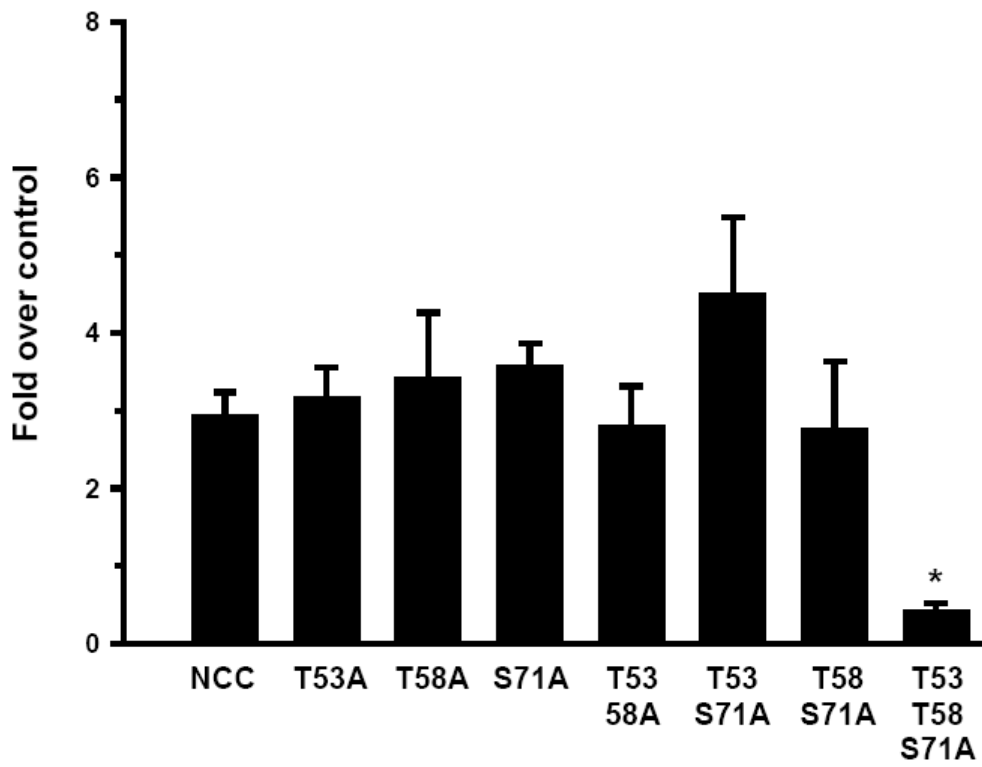


Figure 8

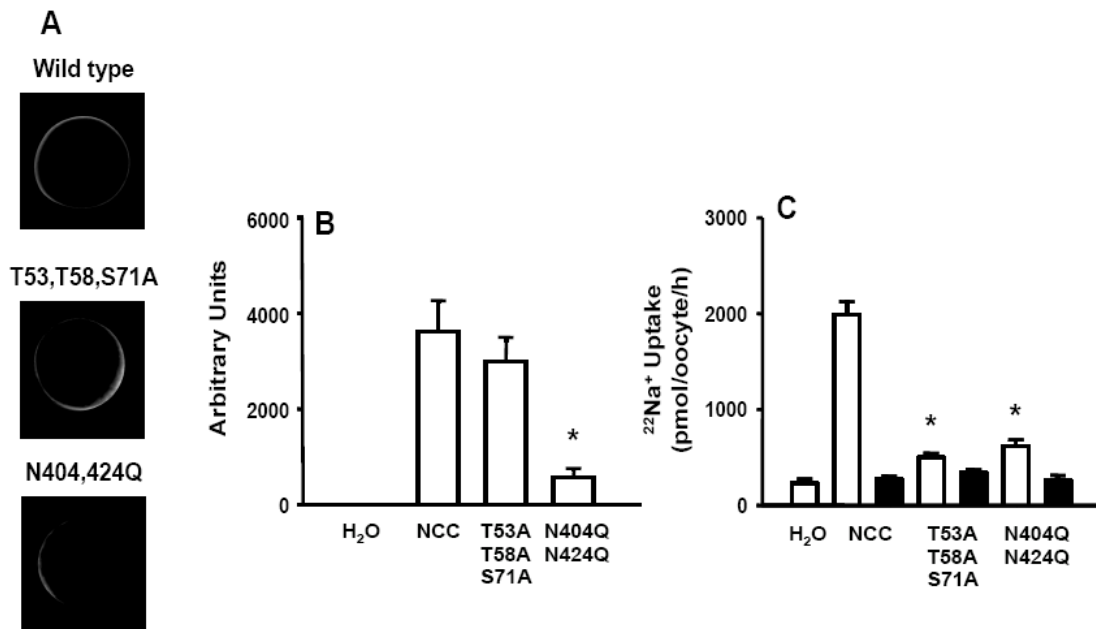


Figure 9

Figures